Pulsed Field Magnetization for GdBaCuO Bulk With Stronger Pinning Characteristics

Hiroyuki Fujishiro, Takuya Hiyama, Takashi Miura, Tomoyuki Naito, Shinya Nariki, Naomichi Sakai, and Izumi Hirabayashi

***Abstract*—The GdBaCuO superconducting bulk with stronger pinning characteristics ($B_T = 1.8$ T at 77 K by the field cooled magnetization (FCM)) has been magnetized at $T_s = 70 - 20$ K by the pulsed field magnetization (PFM) techniques; a sequential pulsed-field application (SPA) and a modified multi pulse technique with stepwise cooling (MMPSC). With decreasing T_s, the pinning force F_P increases especially at the growth sector boundaries (GSBs), and then the nonuniformity of the trapped field profile becomes more and more conspicuous on the bulk surface. At low T_s, the SPA technique is not necessarily a suitable technique to enhance the trapped field B_T and the total trapped flux Φ_T. However, these values can be enhanced by the MMPSC method. The properties of the bulk with stronger pinning characteristics during PFM are discussed.**

***Index Terms*—MMPSC method, pinning force, pulsed field magnetization, trapped field.**

I. Introduction

FOR the practical application of superconducting bulks as a strong quasi-permanent magnet such as a magnetic separation for environmental cleaning [1] and a drug delivery system (DDS) for medical applications [2], the magnetizing technique is very important. Recently, a pulsed field magnetization (PFM) has been developed instead of a conventional field-cooled magnetization (FCM) because of a compact, mobile and inexpensive setup. The trapped field B_T^P by PFM was, however, pretty small, compared with the trapped field B_T^{FC} by FCM due to the large temperature rise by the dynamical motion of the magnetic fluxes. The maximum B_T^P ever reported had been as low as 3.8 T at 30 K by an iteratively magnetizing pulsed-field method with reducing amplitude (IMRA) [3]. We have systematically studied the time and spatial dependences of the temperature $T(t,x)$, local field $B_L(t)$ and the trapped field B_T^P on the surface of cryocooled REBaCuO (RE: rare earth element) bulks during PFM for various starting temperatures T_s and applied fields B_{ex}, and have suggested the importance of the precise measurements of $T(t,x)$ on the bulk surface [4], [5].

To enhance B_T^P, the reduction in temperature rise ΔT is an indispensable issue. The lowering of T_s to 10–20 K, which is effective for FCM due to the enhancement of the critical current density J_c, is not necessarily effective for PFM because of the large heat generation due to the increase of pinning loss and the decrease in the heat capacity of the bulk. Taking the obtained experimental results into consideration, we proposed a new PFM technique named a modified multi pulse technique with stepwise cooling (MMPSC) [6], and have succeeded the highest field trapping of $B_T^P = 5.20$ T on the GdBaCuO bulk?45 mm in diameter, on which only 3.6 T was trapped by a single pulse application at 40 K [7]. $B_T^P = 5.20$ T is a record-high value by PFM to date. We applied the technique to other bulks with different pinning ability and confirmed that the MMPSC was a universal and effective method to enhance B_T^P [8].

Another approach to enhance B_T^P is to use the bulk with higher J_c. Nariki *et al.* have fabricated the high-performance GdBaCuO bulks, on which trapped fields B_T^{FC} were as high as 2.1–2.2 T (48 mm in diameter) [9] and 3.05 T (65 mm in diameter) at 77 K [10]. If the bulk with higher J_c and higher B_T^{FC} is magnetized by PFM such as the MMPSC method, higher B_T^P value is expected. In this paper, we applied the PFM techniques to the GdBaCuO bulk with higher trapped field characteristics ($B_T^{FC} = 1.8$ T at 77 K). The trapped field B_T^P, the total trapped flux Φ_T, and the temperature rise ΔT are investigated for the sequential pulse field application (SPA) and MMPSC methods.

II. Experimental Procedure

The GdBaCuO superconducting bulk disk (45 mm in diameter and 18 mm in thickness) used in this study was fabricated by SRL-ISTEC, Japan. The melt processing was performed under controlled oxygen partial pressure of 1% O_2 in Ar [9]. The trapped field B_T^{FC} was as high as 1.8 T at 77 K. The bulk was mounted on soft iron yoke cylinder and tightly anchored onto the cold stage of a Gifford-McMahon (GM) cycle helium refrigerator. The experimental setup around the bulk was described elsewhere [8]. The magnetizing solenoid coil, which generated the pulse field up to $B_{ex} = 6.4$ T with a rise time of 12 ms and a duration of 100 ms, was placed outside the vacuum chamber, in which the central axis of the resulting field coincides with that of the bulk. The starting temperature T_s of the bulk was controlled over the range from 70 K to 20 K. Three magnetic pulses (Nos. 1–3) with the same amplitude B_{ex} were applied sequentially after re-cooling to T_s. We abbreviate this technique as a sequential pulsed-field application (SPA) method. The time

Manuscript received August 16, 2008. First published June 05, 2009; current version published July 15, 2009. This work was supported in part by a Grant-in-Aid for Scientific Research from the Ministry of the Education, Culture, Sports, Science and Technology, Japan 19560003.

H. Fujishiro, T. Hiyama, T. Miura, and T. Naito are with the Faculty of Engineering, Iwate University, 4-3-5 Ueda, Morioka 020-8551, Japan (e-mail: fujishiro@iwate-u.ac.jp).

S. Nariki, N. Sakai, and I. Hirabayashi are with the Superconductivity Research Laboratory (SRL), International Superconductivity Technology Center (ISTEC), 1-10-13 Shinonome, Koto-ku, Tokyo 135-0062, Japan (e-mail: nariki@istec.or.jp).

Digital Object Identifier 10.1109/TASC.2009.2018081

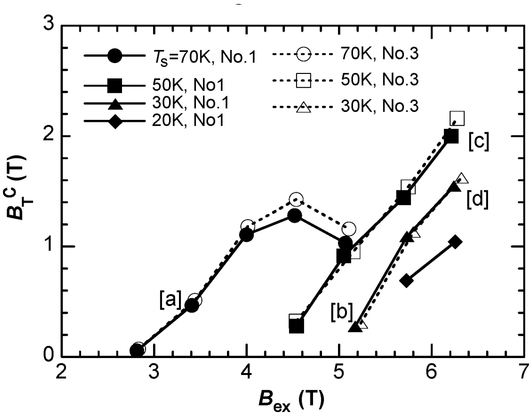

Fig. 1. The trapped field $B_{\rm T}^{\rm C}$ at the bulk center for the No. 1 and No. 3 pulses in the SPA method as a function of the applied pulsed field $B_{\rm ex}$ for various starting temperatures $T_{\rm s}$. In the figure, [a]–[d] denote the typical conditions, at which the $B_{\rm T}$ (0.5 mm) profiles are mapped as shown in Figs. 5(a), 5(b), 6(a), and 6(b), respectively.

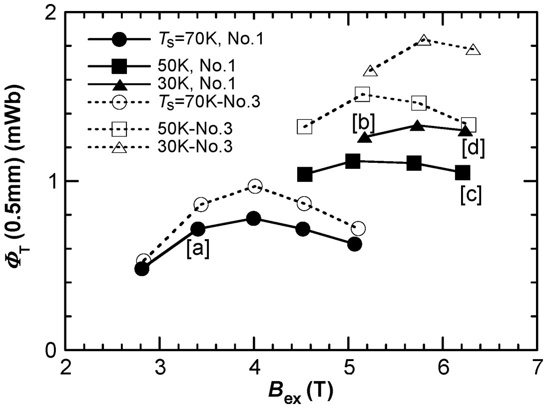

Fig. 2. The total trapped flux $\Phi_{\rm T}$ for the No. 1 and No. 3 pulses in the SPA method as a function of the applied pulsed field $B_{\rm ex}$ for various starting temperatures $T_{\rm s}$. [a]–[d] denote the conditions, at which the $B_{\rm T}$ (0.5 mm) profiles are mapped as shown in Figs. 5(a), 5(b), 6(a), and 6(b), respectively.

dependence of the local field $B_{\rm L}^{\rm C}(t)$ was measured at the bulk center 0.5 mm above the bulk surface, and the temperature $T(t)$ on the bulk surface was also measured using a fine thermocouple during PFM. The trapped field profile $B_{\rm T}$(0.5 mm) was mapped 0.5 mm above the bulk surface, stepwise with a pitch of 1.2 mm by scanning an axial-type Hall sensor (F.W. Bell, BHA 921) inside the vacuum chamber using an $x-y$ stage controller with a flexible bellows. The total amount of the trapped magnetic flux density $\Phi_{\rm T} = \Phi_{\rm T}$ (0.5 mm) was calculated by integrating the magnetic flux density $B_{\rm T}$ (0.5 mm) over the region where it was positive. The MMPSC method was also applied to the bulk. The detailed sequence of the method was described in Section 3.3.

III. Results and Discussion

A. Sequential Pulsed-Field Application (SPA)

Fig. 1 shows the trapped field $B_{\rm T}^{\rm C} = B_{\rm T}^{\rm C}$ (0.5 mm) at the bulk center after the No. 1 and No. 3 pulses in SPA, as a function of the applied pulsed field $B_{\rm ex}$ for various starting temperatures $T_{\rm s}$. For the No. 1 pulse, $B_{\rm T}^{\rm C}$ at $T_{\rm s} = 70$ K starts to increase for $B_{\rm ex} \geq 3$ T, takes a maximum at $B_{\rm ex} = 4.5$ T and then decreases with increasing $B_{\rm ex}$. The $B_{\rm T}^{\rm C} - B_{\rm ex}$ curve can be usually observed for the PFM technique, which is attributed to a temperature rise in the bulk due to the heat generated by the fast motion of flux lines in the presence of resistive forces; the pinning force and the viscous force. The applied pulse field, at which the magnetic flux starts to be trapped at the bulk center, increases to 4.5 T at $T_{\rm s} = 50$ K and further increases with decreasing $T_{\rm s}$. This comes from the increase of the shielding current in the superconductor with decreasing $T_{\rm s}$. The peak in the $B_{\rm T}^{\rm C} - B_{\rm ex}$ curve cannot be confirmed at $T_{\rm s} \leq 50$ K because of the experimental limit of $B_{\rm ex} = 6.4$ T. For the No. 3 pulse, $B_{\rm T}^{\rm C}$ slightly increases as shown in the dotted lines.

Fig. 2 shows the total trapped flux $\Phi_{\rm T}$ after the No. 1 and No. 3 pulse as a function of the applied field $B_{\rm ex}$ for various starting temperatures $T_{\rm s}$. All the $\Phi_{\rm T} - B_{\rm ex}$ curves take a maximum. The maximum $\Phi_{\rm T}$ value increases and the $B_{\rm ex}$ value, at which $\Phi_{\rm T}$ takes a maximum, shifts to the higher value with decreasing $T_{\rm s}$. It should be noted that the $\Phi_{\rm T}$ value fairly increases for the SPA technique; the $\Phi_{\rm T}$ value for the No. 3 pulse is 20∼40% larger than that for the No. 1 pulse, and that the increment rate increases with decreasing $T_{\rm s}$. In this way, the SPA technique is effective for the enhancement of $\Phi_{\rm T}$ rather than that of $B_{\rm T}^{\rm C}$.

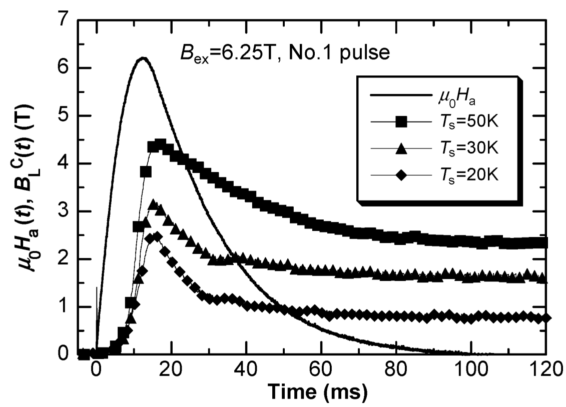

Fig. 3. The time evolution of applied field $\mu_0 H_{\rm a}(t)$ and the local fields $B_{\rm L}^{\rm C}(t)$ after applying the magnetic pulse of $B_{\rm ex} = 6.25$ T at $T_{\rm s} = 50$, 30 and 20 K.

Fig. 3 shows the time evolution of the applied field $\mu_0 H_{\rm a}(t)$ and the local field $B_{\rm L}^{\rm C}(t)$ at the bulk center after applying the No. 1 pulse of $B_{\rm ex} = 6.25$ T at various $T_{\rm s}$. $\mu_0 H_{\rm a}(t)$ was monitored by the current $I(t)$ flowing through the shunt resister using a digital oscilloscope. $B_{\rm L}^{\rm C}(t)$ starts to increase for $t \geq 5$ ms, takes a maximum at 15 ms with a time delay and then decreases to a final value due to the flux flow. The maximum of the $B_{\rm L}^{\rm C}(t)$ is smaller than that of the $\mu_0 H_{\rm a}(t)$, which suggest that $B_{\rm ex} = 6.25$ T is not the enough strength to make the magnetic fluxes intrude into the bulk center at $T_{\rm s} = 50 - 20$ K.

Fig. 4(a) shows the time dependence of the temperature change $T(t)$ on the bulk surface after applying the pulse fields from 5.00 T to 6.32 T at 30 K. $T(t)$ sharply rises up, takes a maximum at 5 s and then gradually decreases. It should be noticed that the time, at which $T(t)$ takes a maximum, is in the order of seconds, which is clear contrast with the local field $B_{\rm L}^{\rm C}(t)$ shown in Fig. 3; the time, at which $B_{\rm L}^{\rm C}(t)$ takes a maximum, is in the order of milliseconds. The maximum temperature $T_{\rm max}$ increases with increasing $B_{\rm ex}$ due to the increase of pinning loss and viscous loss. $T_{\rm max}$ reaches 70 K

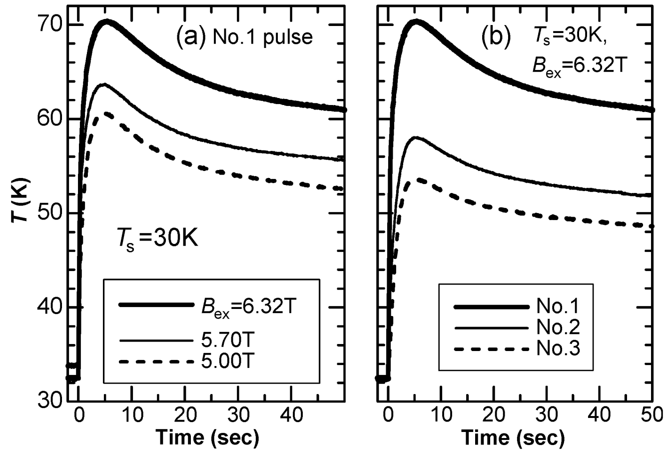

Fig. 4. (a) Time dependence of the temperature change $T(t)$ on the bulk surface after applying the pulse fields from 5.00 T to 6.32 T at 30 K. (b) The pulse number dependence of $T(t)$ on the bulk surface for $B_{\rm ex} = 6.32$ T at 30 K.

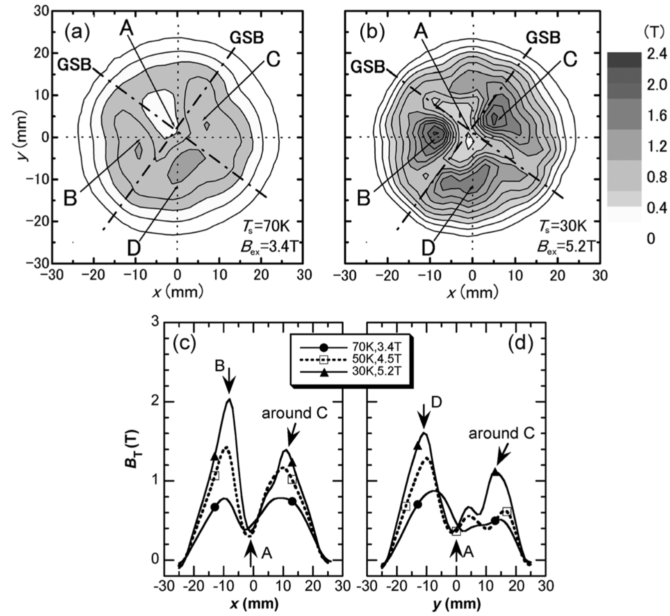

Fig. 5. The trapped field profiles $B_{\rm T}$ (0.5 mm) after applying the pulse field (No.1 pulse) of (a) $B_{\rm ex} = 3.4$ T at $T_{\rm s} = 70$ K and (b) 5.2 T at $T_{\rm s} = 30$ K. The cross sections of the trapped field profiles for typical conditions along the (c) x- and (d) y-axes, respectively

for $B_{\rm ex} = 6.32$ T. The maximum temperature rise $\Delta T_{\rm max}$ increased with decreasing $T_{\rm s}$ (not shown) due to the enhancement of pinning loss and the decrease in the heat capacity of the bulk. Fig. 4(b) shows the pulse number dependence of $T(t)$ in the SPA method on the bulk surface for $B_{\rm ex} = 6.32$ T at $T_{\rm s} = 30$ K. $T_{\rm max}$ gradually decreases with increasing pulse number and then saturates due to the decrease of the pinning loss of the already trapped fluxes. The decrease of the $T_{\rm max}$ enhances the $\Phi_{\rm T}$ and $B_{\rm T}^{\rm C}$ values as shown in Figs. 1 and 2.

Figs. 5(a) and 5(b) show the trapped field profiles $B_{\rm T}$ (0.5 mm) after applying the No. 1 pulse field of $B_{\rm ex} = 3.4$ T at $T_{\rm s} = 70$ K and $B_{\rm ex} = 5.2$ T at $T_{\rm s} = 30$ K, respectively. For relatively higher $T_{\rm s}$ and lower $B_{\rm ex}$, as shown in Fig. 5(a), the nonuniformity of the trapped field profile is not so large, except for the region near the position A. The result roughly suggests that the distribution of $J_{\rm c}$ in the bulk is relatively small at higher $T_{\rm s}$. On the other hand, at lower $T_{\rm s}$ and relatively lower $B_{\rm ex}$, as shown in Fig. 5(b), the position dependence of the trapped field is quite remarkable; $B_{\rm T}$ at the positions B, C and D increases over 1.5 T. However, $B_{\rm T}$ at the position A (bulk center) remains 0.5 T. The positions B, C and D are not in the growth sector boundaries (GSBs) but in the growth sector regions (GSRs). The pinning force in the GSBs is usually stronger than that in the GSRs due to the large number of crystal defects. The nonuniformity of the trapped field might be a characteristic feature for the bulk with strong pinning force. Figs. 5(c) and 5(d) show the cross sections of the trapped field profiles for typical conditions along the x- and y-axes, respectively, in which the characteristic positions from A to D are indicated. $B_{\rm T}$ at the positions B, D and around C increases with decreasing $T_{\rm s}$. For the lower $B_{\rm ex}$, the magnetic fluxes can be preferentially trapped at the weak pinning centers in the GSRs.

Figs. 6(a) and 6(b) show the $B_{\rm T}$ (0.5 mm) profile after applying the higher pulse field (No.1 pulse) of $B_{\rm ex} = 6.2$ T at $T_{\rm s} = 50$ K and 30 K, respectively. In Fig. 6(a), the $B_{\rm T}$ shows nearly the cone-shaped profile and the magnetic fluxes are preferentially trapped along the GSBs rather than the positions B, C and D. As a result, the center of the trapped field shifts toward the bulk center (position A). In this way, for the higher

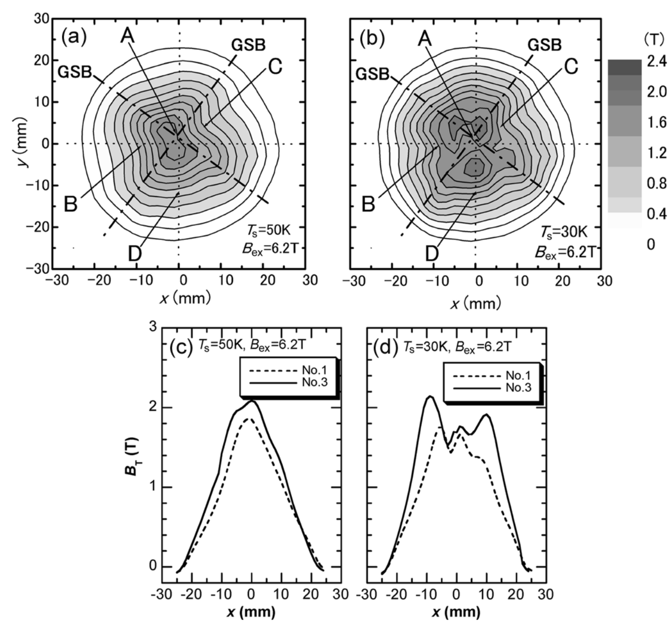

Fig. 6. The trapped field profiles $B_{\rm T}$ (0.5 mm) after applying the pulse field (No.1 pulse) of (a) $B_{\rm ex} = 6.2$ T at $T_{\rm s} = 50$ K and (b) 6.2 T at $T_{\rm s} = 30$ K. The cross sections along the x-axis of the trapped field profiles after applying the (c) No. 1 and (d) No. 3 pulse field of $B_{\rm ex} = 6.2$ T, respectively.

$B_{\rm ex}$, the magnetic fluxes can be preferentially trapped at the strong pinning centers in the GSBs due to the large temperature rise. Figs. 6(c) and 6(d) show the cross section of the $B_{\rm T}$ profile along the x-axis for No. 1 and No. 3 pulses of $B_{\rm ex} = 6.2$ T at $T_{\rm s} = 50$ K and 30 K, respectively. It should be noted that the trapped fields are enhanced especially at the bulk periphery by the SPA method.

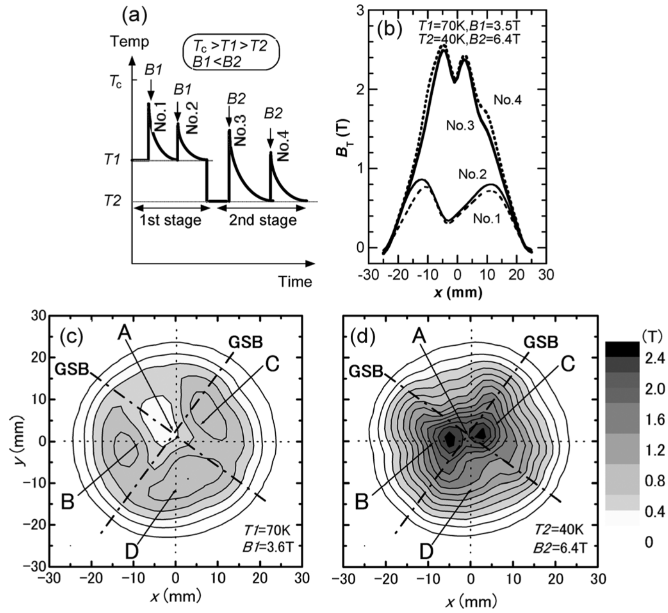

Fig. 7. (a) The estimated time dependence of temperature $T(t)$ in the MMPSC method. (b) The measured cross section of the B_T (0.5 mm) profiles for each step in the MMPSC method. The B_T (0.5 mm) profiles after applying the (c) No. 2 pulse and the (d) No. 3 pulse in the MMPSC method.

B. MMPSC Method

Fig. 7(a) shows the conception of the MMPSC method [6]. Four magnetic pulses were applied at different initial temperatures $T_s = T1$ and $T2$. At the first stage, a lower pulse field of $B1 = 3.5$ T was applied twice (No. 1 and No. 2) at $T1 = 70$ K in order to realize the "M-*shaped*" trapped field profile on the bulk surface, which means the lower trapped field at the bulk center than that at the bulk periphery, and is necessary to enhance the final B_T^P [6], [7]. At the second stage, the bulk was cooled down to $T2 = 40$ K and a higher pulse field of $B2 = 6.4$ T was applied twice (No. 3 and No. 4). A small and proper amount of magnetic fluxes should be trapped on the bulk periphery for the reduction in ΔT at a first stage at $T1$, and the strong and optimum pulse field $B2$ should be applied at a second stage at $T2$.

Fig. 7(b) shows the cross section of the B_T (0.5 mm) profile along the x-axis for each step in the MMPSC method. At the first stage, the "M-*shaped*" trapped field profile can be obtained, and at the second stage, B_T as high as 2.6 T and $\Phi_T(0.5\ \mathrm{mm}) = 1.60\ \mathrm{mWb}$ were realized, which were higher than those obtained by the SPA method as shown in Fig. 1. Figs. 7(c) and 7(d) show the B_T (0.5 mm) profiles of the No. 2 pulse and the No. 3 pulse in the MMPSC method, respectively. After the No. 3 pulse application, the magnetic fluxes are preferentially trapped along the GSBs rather than along the GSRs, where the positions B, C and D exist.

IV. Summary

The GdBaCuO superconducting bulk with excellent field trapping ability ($B_T = 1.8$ T at 77 K by the field cooled magnetization (FCM)) has been magnetized by a sequential pulsed-field application (SPA) and a modified multi pulse technique with stepwise cooling (MMPSC). With decreasing temperature, the pinning force F_P increases especially at the growth sector boundaries (GSBs) rather than the growth sector regions (GSRs), and then the nonuniformity of the trapped field distribution becomes more and more conspicuous on the bulk surface. It was found that the MMPSC method was valuable technique to enhance the trapped field B_T^C and the total trapped fluxes Φ_T also for the bulk with stronger pinning characteristics. However, since the optimum condition for the MMPSC method strongly depends on the used bulk crystal and the experimental apparatus, it is not easy to apply the MMPSC method. The advent of a new PFM technique is anticipated to magnetize sufficiently the superconducting bulks with stronger pinning characteristics.

Acknowledgment

The authors would like to thank Y. Yanagi and Y. Itoh of IMRA Materials R&D Co., Ltd., Japan, for valuable discussion and for the technical support for the measurement apparatus of the trapped field distribution.

References

[1] H. Hayashi, K. Tsutsumi, N. Saho, N. Nishizima, and K. Asano, "Study on a mobile-type magnetic separator applying high- T_c bulk superconductors," *Phys. C*, vol. 392–396, pp. 745–748, 2003.

[2] F. Mishima, S. Takeda, Y. Izumi, and S. Nishijima, "Development of magnetic field control for magnetically targeted drug delivery system using a superconducting magnet," *IEEE Trans. Appl. Supercond.*, vol. 17, pp. 2303–2306, 2006.

[3] Y. Yanagi, Y. Itoh, M. Yoshikawa, T. Oka, T. Hosokawa, H. Ishihara, H. Ikuta, and U. Mizutani, "Trapped field distribution on Sm-Ba-Cu-O bulk superconductor by pulsed-field magnetization," in *Advances in Superconductivity XII*. Tokyo, Japan: Springer-Verlag, 2000, pp. 470–474.

[4] H. Fujishiro, K. Yokoyama, M. Kaneyama, T. Oka, and K. Noto, "Effect of metal ring setting outside HTSC bulk disk on trapped field and temperature rise in pulse field magnetizing," *IEEE Trans. Appl. Supercond.*, vol. 15, pp. 3762–3765, 2005.

[5] H. Fujishiro, M. Kaneyama, K. Yokoyama, T. Oka, and K. Noto, "Rise-time elongation effects on trapped field and temperature rise in pulse field magnetization for high temperature superconducting bulk," *Jpn. J. Appl. Phys.*, vol. 44, pp. 4919–4925, 2005.

[6] H. Fujishiro, M. Kaneyama, T. Tateiwa, and T. Oka, "Record-high trapped magnetic field by pulse field magnetization using GdBaCuO bulk superconductor," *Jpn. J. Appl. Phys.*, vol. 39, pp. L1221–L1224, 2005.

[7] H. Fujishiro, T. Tateiwa, A. Fujiwara, T. Oka, and H. Hayashi, "Higher trapped field 5 T on HTSC bulk by modified pulse field magnetizing," *Phys. C*, vol. 445–448, pp. 334–338, 2006.

[8] H. Fujishiro, T. Tateiwa, and T. Hiyama, "Enhancement of trapped field and total trapped flux on high temperature bulk superconductor by a new pulse-field magnetization method," *Jpn. J. Appl. Phys.*, vol. 46, pp. 4108–4112, 2007.

[9] S. Nariki, M. Fujikura, N. Sakai, I. Hirabayashi, and M. Murakami, "Field trapping and magnetic levitation performances of large single-grain Gd-Ba-Cu-O at different temperatures," *Physica C*, vol. 426–431, pp. 654–659, 2005.

[10] S. Nariki, N. Sakai, and M. Murakami, "Melt-processed Gd-Ba-Cu-O superconductor with trapped field of 3 T at 77 K," *Supercond. Sci. Technol.*, vol. 18, pp. S126–S130, 2005.